


 Cite this: *RSC Adv.*, 2020, 10, 21108

Unbound water in mechanochemical reactions of brown coal

 Tatiana Skripkina,^{ID}* Artem Ulihin, Aleksey Bychkov,^{ID} Sergey Mamylov,^{ID} Ekaterina Podgorbunskikh,^{ID} Igor Lomovskiy^{ID} and Oleg Lomovsky^{ID}

Mechanochemical activation of coal is commonly employed in industry. However, even the simplest solid-phase reactions, such as neutralization of humic acids in brown coal, remain insufficiently studied. The hypothesis regarding the occurrence of mechanochemical neutralization under local hydrothermal conditions for humic acids in brown coal has been tested in this study. 3D modelling of the "block–interlayer" system (where coal particles are separated by air interlayers saturated with water vapor) was used. The 3D model showed that the permittivity is expected to rise from 14 to 16% as the moisture content in the system increases from 12 to 15%. The actual permittivities of coal with different moisture contents have been measured by dielectric spectroscopy. In the real system, the permittivity increases more than threefold as the moisture content rises from 12 to 15%. This increase is much greater than the calculated one, demonstrating that the phase containing unbound water appears in the system at a moisture content of ~12–13% and may exert various effects on the solid-phase reaction. There is a correlation between the moisture content, permittivity, and predominant mechanisms of the reaction between the organic matter in brown coal and sodium percarbonate (a reagent simultaneously containing the alkaline and peroxidic components). The reactions between brown coal and alkaline reagents proceed under local hydrothermal conditions. Both the alkaline and peroxidic components of sodium percarbonate participate in the solid-phase reaction between brown coal and sodium percarbonate. The emergence of unbound water in coal significantly inhibits the oxidation reaction.

 Received 7th April 2020
 Accepted 26th May 2020

DOI: 10.1039/d0ra03131c

rsc.li/rsc-advances

Introduction

Mechanochemical treatment of coal is employed in the power industry,^{1,2} carbon chemistry,³ pharmaceuticals,^{4,5} and agriculture, including manufacturing of feed additives for cattle and products for soil amelioration and stimulation of plant growth.⁶ Mechanochemical technologies are considered to be eco-friendly because they are highly efficient and allow one to use fewer manufacturing stages, while not using solvents.^{7,8} During mechanochemical treatment of brown coal, chemical reactions usually immediately follow the mechanical activation of brown coal and the reactions occurring directly in the mechanochemical solution.⁹ Vigorous interaction is known to activate the coal organic matter, which significantly alters its physicochemical properties.^{10,11} The mechanically activated (MA) coals are characterised by an enhanced reactivity during the subsequent treatment with reagents, resulting in higher yields and contents of various extractable substances, higher conversion degree of coal organic matter during thermal and supercritical dissolution, as well as during hydrogenation.^{12,13} Mechanical activation of coal leads to particle disintegration, up to the

particle size of several dozen micrometers.¹⁴ This is accompanied by an increase in free surface area, pore opening, and vigorous electrification that is proportional to the number of paramagnetic centres in coal. Mechanical activation (MA) of dry coals was found to significantly increase the concentration of paramagnetic centres.^{15,16}

Humic acids, with their content in fossil fuel being as high as 80%, are the key biologically active compounds and are of the greatest interest for industrial applications. Mechanochemical treatment of brown coal with alkalis (*e.g.*, sodium and potassium hydroxides) has been most commonly used in industry. The content of water-soluble humic substances in the resulting product is 3–5-fold higher than that in the untreated coal.¹⁷ This can be explained by neutralization that takes place during treatment: humic acids are converted to the water-soluble form of sodium humate during this process. In order to verify this assumption, it is important to study the role played by water in these processes.

Mechanochemical treatment of brown coal in the presence of sodium percarbonate is of special interest, since this reagent contains both the alkaline and the peroxidic components. The interaction between brown coal and sodium percarbonate is known to involve oxidation of the organic matter in brown coal, which enhances the extractability of humic acids, increases the

Institute of Solid State Chemistry and Mechanochemistry SB RAS, Novosibirsk, 630128, Russia. E-mail: skripkina.t.s@gmail.com



contents of phenolic and carboxylic groups,^{18–20} and improves the sorption properties of the product.^{21,22} Hydrogen peroxide within sodium percarbonate can act as a source of free radicals; oxidation of brown coal with sodium percarbonate proceeds *via* the water-dependent free-radical mechanism.²³

The objective of this study was to investigate the effect of moisture content on the mechanochemical reactions between brown coal and alkaline or alkaline oxidising agents.

Experimental

Brown coal from the Itatskoye deposit of the Kansk-Achinsk coal basin (Russia) was used as raw material.

The moisture contents in the samples were measured gravimetrically by drying to a constant weight (weight difference of <0.1% observed for 3 min) at 130 °C on a RADWAG WPS 50 SX moisture analyzer using a halogen lamp as a heating element.

X-ray diffraction analysis was conducted on a D8 Advance diffractometer (Bruker, Germany) using CuK α radiation in the Bragg–Brentano geometry. The XRD patterns were analyzed using the ICDD PDF-2 database. The particle size distribution and the width/length distribution of brown coal were determined using a CAMSIZER X2 instrument (Retsch Technology GmbH, Germany) that captures the projections of the analyzed particles with digital cameras. The measurements were conducted using an X-Jet module, where particles were dispersed under air pressure of 75 kPa. The volume-based particle size distribution Q was plotted using xc_min (width), which displays the particle width that is determined from the narrowest of all the measured chords for each particle projection. The width/length ratio b/l was determined as $b/l = xc_min/xFe_max$, where xFe_max (length) is the largest Feret diameter in the measured set of Feret diameters of a particle.

The specific surface area of the samples was determined by nitrogen thermal desorption on a Sorbtometer M analyzer (Catacon, Russia) using the BET theory²⁴ and the approximations proposed by Gregg and Sing.²⁵

The contents of alkali-soluble and water-soluble humic acids were measured according to the State Standard GOST 9517-94 (ISO 5073:2013).

Mechanochemical activation of a mixture of brown coal and the reagents (10 g) was carried out in an AGO-2 laboratory-type planetary mill equipped with a water cooling system. The weight of grinding balls loaded into the mill was 200 g; acceleration of the grinding bodies at the instant when they detached from the grinding chamber walls was 200 m s⁻²; the exposure time was 2 min. Moisture content in the original raw material was a variable being changed from 0 to 30%. When coal was treated in the presence of sodium percarbonate, the dry matter content of the reagent was 5%. When coal was subjected to mechanochemical activation in the presence of sodium carbonate, the content of the reagent was equivalent to that of sodium percarbonate in the respective parallel experimental run. Mechanical activation of dry brown coal without any reagents added was carried out in a similar manner.

3D modelling of the “block–interlayer” system (brown coal particles separated by air interlayers, which were subsequently

saturated with water vapor) was conducted. The particles were merged into blocks with the maximum dimensions corresponding to mesh size. Under an assumption that the particles had an isometric structure, their dimensions were determined from the nitrogen adsorption data according to the intergrain and intrapore components of the specific surface area. The roughly estimated particle (grain) size was 2 μm ; the interlayer thickness was 5–20% of grain size. The dimension parameters within the model were varied from several fractions of a micrometer to several micrometers.

The modelling was conducted using the Monte-Carlo method. The results of 3D modelling were presented as curves showing a degree to which water filled the interlayer volume as a function of time. The curves have a typical sigmoid shape and demonstrate that the initial vigorous filling is followed by a plateau when there are no more vacant places where water could be adsorbed in the system. A family of curves was plotted for the expanding system as the lattice parameter increased. At each stage of water adsorption, we calculated the permittivity of the composite as a system of capacitors connected in series and parallel combinations.

The permittivities of the coal samples having different moisture contents were measured using a Precision LCR Meter HP4284A analyzer of electrophysical properties operating at fixed frequencies (1 MHz and 100 Hz). The samples were pressed into pellets with copper electrodes inserted into their butt ends under a pressure of 6.5 MPa cm⁻². The permittivities were calculated according to the measured data taking into account the geometric parameters of the samples.

Results and discussion

Analysis of coal before and after mechanical activation

The X-ray diffraction patterns of the coal samples contain (002), (100), and (110) lines related to graphite at $2\theta = 24^\circ$ – 25° , 40° – 43° , and 80° , respectively. The first peak corresponds to the distance between graphite planes.²⁶ The (002) reflection is ascribed to diffraction from the equidistant graphite layers. The XRD patterns of high-carbon coals such as anthracite (96 wt% carbon) are most similar to those of graphite and have well defined individual reflections of graphite. As the degree of coalification decreases (*e.g.*, when proceeding from anthracite to lignite (65 wt% carbon)), the XRD patterns become more and more diffuse, and the (002) reflection is shifted towards smaller diffraction angles.^{27,28} Fig. 1 shows the XRD patterns of the initial mechanochemically activated brown coal samples. A comparison of the XRD patterns showed that the (002) peak corresponding to graphite layers (at $2\theta = 24^\circ$ – 25°) presumably resulted from amorphization of brown coal during mechanical activation.

Fig. 2 shows that the average width/length ratio of the brown coal samples increases after mechanochemical activation: from 0.75 to 0.79 for the samples activated for 1, 2 and 3 min and from 0.75 to 0.78 for the sample subjected to 5 min activation. The particle size changes in the same manner. After mechanical activation, the average particle size decreases down to the grinding limit ($\sim 14.5 \mu\text{m}$) already after activation

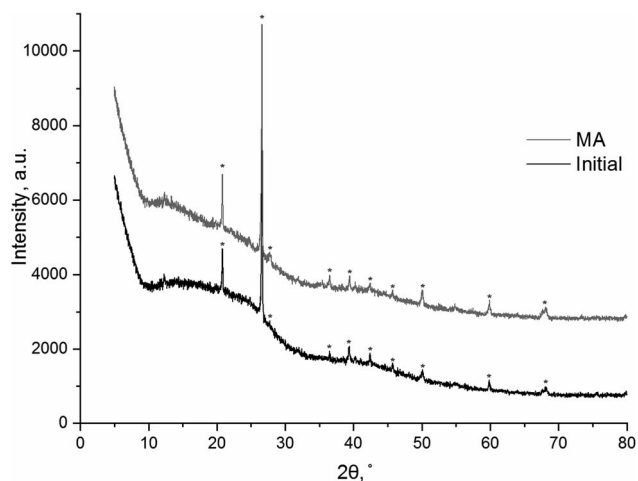


Fig. 1 XRD patterns of the initial and mechanically activated brown coal samples. An asterisk shows the reflections of quartz SiO_2 (PDF no. 01-070-7344).

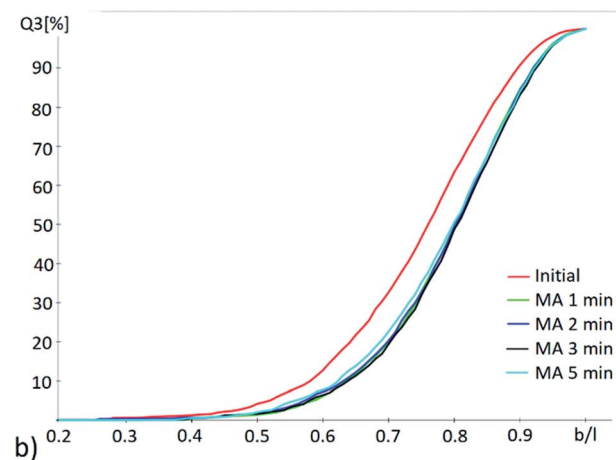
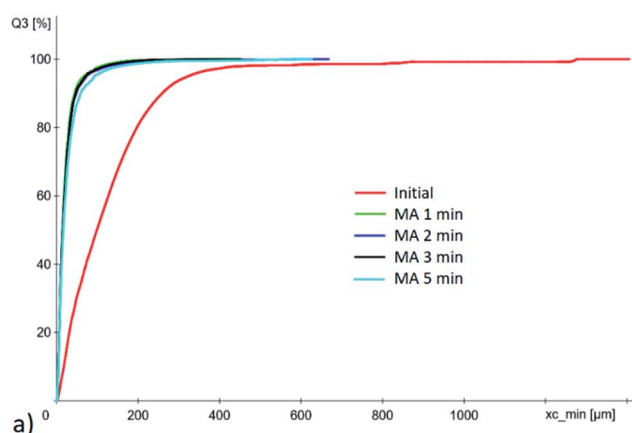


Fig. 2 (a) Cumulative particle size distribution and (b) cumulative width/length distribution of the brown coal samples before and after mechanical activation of different duration.

for 1 min. Particle size was not further decreased at longer duration of mechanical activation. After the activation for 5 min, the average particle size somewhat increased ($\sim 16.5 \mu\text{m}$) due to partial particle aggregation.

Although the grinding limit was reached after mechanical activation for 1 min, the depth of chemical reactions of brown coal both with alkali and alkaline-oxidising reagents rose as the duration of mechanical activation was increased to 2 minutes. For example, after the air-dried brown coal with sodium percarbonate was subjected to 1 min treatment, the yield of water-soluble humic acids increased from 1 to $6.8 \pm 0.2\%$ and reached $9.9 \pm 0.4\%$ after 2 min. The further increase in duration of mechanical activation did not elevate the yield of humic acids and led to excessive loss of energy consumed for processing. To ensure correct comparison of the results, the 2 min duration of mechanical treatment was further used for the discussion.

Fig. 3 shows the isotherms of nitrogen adsorption onto the untreated and mechanically activated brown coal samples. Mechanical treatment altered the surface properties of the product. The shape of the isotherm for untreated brown coal corresponds to type II isotherm, which is typical of adsorption onto nonporous or macroporous adsorbents (Fig. 3a). The shape of the isotherms for mechanically activated brown coal corresponds to polymolecular adsorption onto mesoporous adsorbents with a typical hysteresis loop (the type IV isotherms). The shape of the hysteresis loop demonstrates that the sample contains slit-like pores (Fig. 3a). The external surface of mesoporous particles of the untreated brown coal sample is $0.6 \text{ m}^2 \text{ g}^{-1}$.

The adsorbent-adsorbate interaction forces, monolayer capacity, and the specific surface area (SSA) increase in the mechanically activated sample (Table 1).

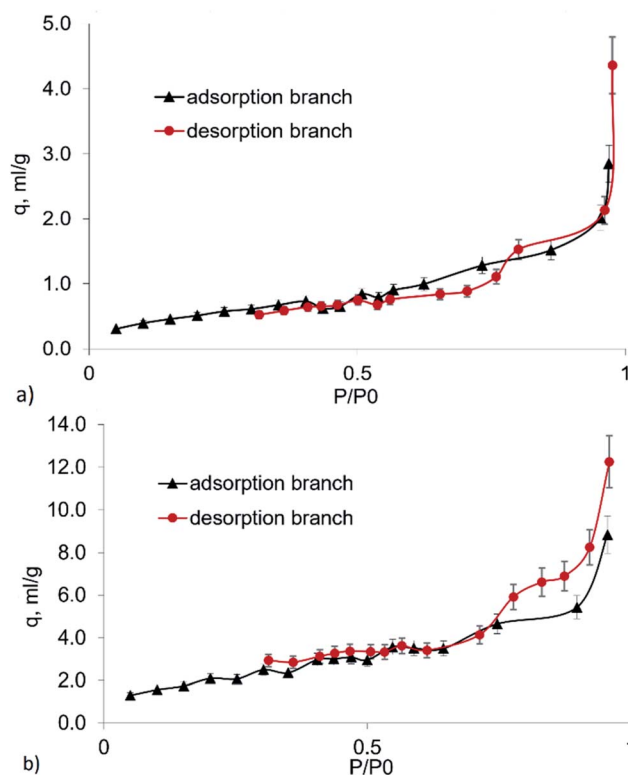


Fig. 3 The isotherm of nitrogen adsorption onto the (a) untreated and (b) mechanically activated brown coal samples.

Modelling the electromagnetic properties of coal depending on moisture content

The determined particle size values were used for 3D modelling of properties of the brown coal–water system. As earlier demonstrated in a number of studies, the water phase plays a crucial role in the course of solid-phase mechanochemical reactions.^{29–32} As moisture content in a substance increases, bound water becomes free (unbound). The unbound water has a high permittivity. The isometric model consisted of brown coal particles separated by air interlayers, which subsequently adsorbed water. The resulting blocks were merged into macroparticles, whose dimensions were determined by sieve analysis (400 μm). A model showing how the permittivity of a macroparticle changes with increasing moisture content was built. In this model, the permittivity of the composite as a system of capacitors connected in series and parallel combinations was calculated at each stage of water adsorption. The modelled correlation shows that the permittivity increases linearly from 9 to 22 as coal moisture rises from 4.5 to 23.5%. Within the 12–15% range of moisture contents, the permittivity is expected to change from 14 to 16.

Experimental determination of the permittivity of coal

In our experiments, brown coal samples with different moisture contents were pressed into pellets, which can be regarded as capacitors with certain capacitance that can be converted into permittivity units. The capacitance of a capacitor filled with the analysed substance as a function of moisture content in the sample was studied experimentally in different frequency ranges. In order to determine the potential influence of polarization and sample geometry, control measurements were conducted at a frequency of 1 MHz. Fig. 3 shows the relative permittivity of brown coal as a function of its moisture content.

Fig. 4 demonstrates that when oscillation frequency of an electric field intensity vector is 100 Hz, the permittivity differs from that obtained at 1 MHz by one order of magnitude. This difference can be caused by the fact that water molecules existing in the relatively “free” state (water molecules are either not bound to the material or bound to it very weakly) acquire a certain orientation at a frequency of 1 MHz. However, the number of these molecules is noticeably smaller than that of “bound” water molecules. The abrupt rise in permittivity at 100 Hz and 1 MHz implies that the maximum degree of saturation of brown coal with water is 12–15%. At higher concentrations, water in the sample exists in its “free” (unbound) form.

The permittivity of the samples rises as moisture content increases from 0 to 13%. At a moisture content of $\sim 13\%$, the

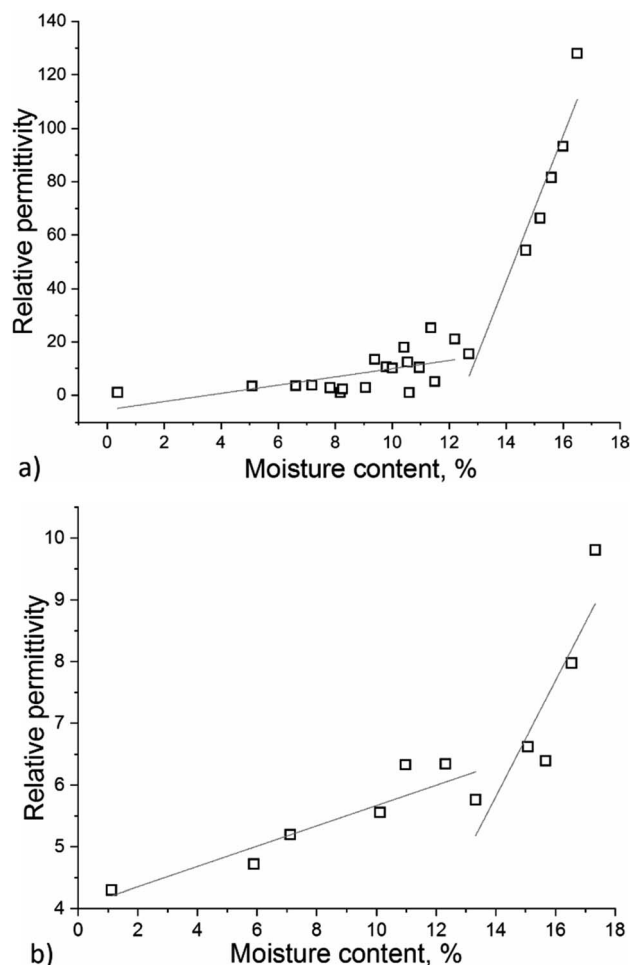


Fig. 4 Relative permittivity of brown coal samples depending on moisture content at frequency of the electromagnetic field 100 Hz (a) and 1 MHz (b).

permittivity starts to increase more rapidly, thus indicating that the mobility of water dipoles in the sample has changed and agglomerates of water molecules have been formed. In the model system, the permittivity increases from 14 to 16 (by 14.3%) as moisture content rises from 12 to 15%. In the real system, permittivity increases more than threefold, which is much greater than the calculated values. This fact indicates that although there was no percolation effect, water exists in a more mobile state and is accumulated nonrandomly.

A conclusion can be drawn from the reported results that the water phase appears in the reaction mixture when moisture content in coal is $\geq 13\text{--}15\%$.

Table 1 Surface properties of the untreated and mechanically activated brown coal

Sample	C_{BET}	Monolayer capacity a_m , mg l^{-1}	SSA, $\text{m}^2 \text{g}^{-1}$ (BET method)	SSA, $\text{m}^2 \text{g}^{-1}$ (according to Gregg and Sing)
Untreated brown coal	28.30	0.51	2.1 ± 0.1	3.0 ± 0.2
MA brown coal	50.48	1.96	7.4 ± 0.4	9.6 ± 0.6

The contribution of unbound water to the mechanochemical reactions

Table 2 shows the changes in acid–base properties (pH) of the mixtures of coal with various reagents before and after mechanical activation. Alkaline reagents present in the initial mixtures increase pH of aqueous suspensions prepared using these mixtures. The alkaline reagents are consumed during treatment. That is why the mechanically activated mixture has a lower pH. Mechanochemical treatment of brown coal and peat performed in order to enhance the extractability of humic acids typically involves a solid-phase reaction with alkalis (mostly with sodium hydroxide). The effect of this treatment is based on conversion of the protonated form of humic acids to sodium humate, which is more soluble.

This process is also expected to take place during the reaction between the organic matter of coal and sodium percarbonate, which contains both the alkaline and the oxidising components. Treating brown coal with both sodium hydroxide and sodium percarbonate significantly increases the yield of water-soluble humic acids. The initial coal sample contains ~1% of water-soluble humic acids, 25% of alkali-soluble humic acids extractable *via* complete alkaline extraction, and 10.7% of ash. It was shown earlier that after treatment under optimal conditions, the yields of alkali and water soluble extracts of humic substances increase to 72% and 15%, respectively.²² However, the contents of phenolic and carboxylic functional groups can be increased by treating coal with sodium percarbonate. The IR spectra of humic acids in brown coal subjected to mechanochemical treatment with sodium percarbonate contained a pronounced band at 1710–1725 cm⁻¹ (the C=O group mainly in carboxyl groups), which was not detected separately in the sample isolated from initial brown coal.²³ The contents of phenolic (Ar–OH) and carboxyl groups (the total number of Ar–COOH and Alk–COOH) in brown coal subjected to mechanochemical activation in the presence of sodium percarbonate are higher than those in untreated coal by 55 and 103%, respectively.²¹ Exposure to sodium hydroxide does not change the content of functional groups in coal, since this reaction proceeds only *via* the acid–base mechanism.

Parallel experimental runs, where brown coal was subjected to mechanochemical activation in the presence of equivalent amounts of sodium percarbonate and sodium carbonate, were conducted in order to determine the role played by the acid–

base mechanism in the reaction between brown coal and sodium percarbonate. The dependence between the yield of water-soluble humic acids and moisture content in brown coal elucidated in these experiments (Fig. 5) allows one to draw some conclusions regarding the differences in the mechanisms of the processes occurring during the reaction.

When the moisture content in coal is ~13%, the yields of water-soluble humic acids in the reactions with sodium percarbonate and sodium carbonate are almost identical. When coal is subjected to treatment in the presence of sodium carbonate, higher moisture content increases the yield of HAs. An opposite effect is observed during treatment in the presence of sodium percarbonate: lower yields are reached at higher moisture contents, while the highest reaction efficiency and a much higher yield of humic acids are observed at moisture content below 12–13%. Unbound water facilitates the reaction with sodium carbonate and, conversely, inhibits the reaction with sodium percarbonate. This difference demonstrates that the oxidising agent (hydrogen peroxide within sodium percarbonate) present in the mixture alters the reaction mechanism and increases the yield of water-soluble humic acids.

The fact that the organic matter of brown coal interacts with sodium carbonate is consistent with the classical model of solid-phase neutralization reactions under local hydrothermal conditions.^{33–36} When using sodium percarbonate as a reagent, the reaction can proceed *via* different mechanisms depending on moisture content in the system. It is fair to assume that if a system contains free (unbound) water, the reaction proceeds due to the alkaline component of sodium percarbonate and is equivalent to neutralization reaction under local hydrothermal conditions. At low moisture content in the system (<12–13%), water exists in the bound state, and the peroxidic component of sodium percarbonate is involved in the reaction. This component triggers the radical-mediated oxidation mechanism and causes oxidation of brown coal, which gives rise to new oxygen-containing functional groups.^{37,38}

The effect of moisture content on the course of a mechanochemical reaction is especially important for technology scale-up, which is a complex process where many parameters need to be

Table 2 Changes in pH of the mixture of reagents after mechanical activation

	pH of the 1 : 10 suspension in water	
	Before MA	After MA
Brown coal without additives	5.4	5.4
Brown coal + Na ₂ CO ₃	10.5	7.0
Brown coal + NaOH	11.7	8.7
Brown coal + 2Na ₂ CO ₃ ·3H ₂ O ₂	10.4	7.3

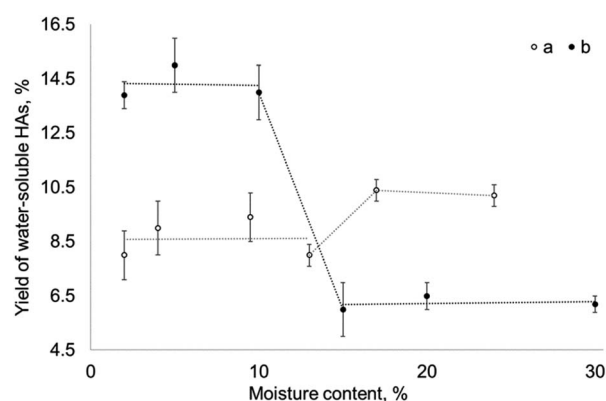


Fig. 5 Efficiency of the mechanochemical reaction of brown coal with (a) sodium carbonate and (b) sodium percarbonate depending on moisture content.

taken into account.^{39,40} The presence of a large amount of unbound water during mechanical activation may cause unstable operation mode, which can be as severe as hardening of the reaction mixture and equipment failure.⁴¹ An additional advantage of using the reaction between brown coal and sodium percarbonate is that it is successfully completed at low moisture contents in the system, unlike treatment of coal with alkalis, which is currently commonly used and poses a problem for scaling up the technology of mechanochemical activation of coal.

Conclusions

It has been demonstrated that permittivity analysis is a simple and very efficient tool to detect unbound water in the system. The reactions between brown coal and alkaline reagents proceed under local hydrothermal conditions. Both the alkaline and peroxidic components of sodium percarbonate are involved in its solid-phase reaction with brown coal. When the system contains no unbound water, the reaction proceeds *via* the radical-mediated oxidation mechanism caused by the presence of hydrogen peroxide within sodium percarbonate. The emergence of unbound water in coal significantly impedes the radical-mediated oxidation reaction. When setting up the technology where a new raw material is used, its permittivity needs to be measured at different moisture contents to identify the point above which unbound water appears in the system.

Conflicts of interest

The authors declare no conflicts of interest.

Acknowledgements

The study of permittivity, 3D modelling, mechanochemical experiments and X-ray diffraction analysis were supported by the Russian Science Foundation [project no. 16-13-10200]. The measurements of the surface properties of coal before and after mechanical activation were carried out within the state assignment to the Institute of Solid State Chemistry and Mechanochemistry, Siberian Branch of the Russian Academy of Sciences (project no. AAAA-A17-117030310279-0).

Notes and references

- 1 A. P. Burdukov, E. B. Butakov, A. V. Kuznetsov and M. Y. Chernetskiy, *Explos. Shock Waves*, 2018, **54**, 20–23.
- 2 J. Li, Z. Li, Y. Yang, C. Wang and L. Sun, *Powder Technol.*, 2018, **339**, 102–110.
- 3 P. Baláž and E. Dutková, *Miner. Eng.*, 2009, **22**, 681–694.
- 4 L. Turčániová, J. Kádárová, P. Imrich, T. Liptaj, J. Vidlár, J. Vašek, F. Foldyna, J. Sitek and P. Baláž, *J. Mater. Sci.*, 2004, **39**, 5467–5470.
- 5 V. V. Boldyrev, *J. Mater. Sci.*, 2004, **39**, 5117–5120.
- 6 N. V. Yudina, A. V. Savel'eva and E. V. Linkevich, *Solid Fuel Chem.*, 2019, **53**, 29–35.
- 7 A. Agarwal, M. Rana and J.-H. Park, *Fuel Process. Technol.*, 2018, **181**, 115–132.
- 8 H. Liu, Y. Zhang, T. Hou, X. Chen, C. Gao, L. Han and W. Xiao, *Fuel Process. Technol.*, 2018, **174**, 53–60.
- 9 A. Bychkov, E. Podgorbunskikh, E. Bychkova and O. Lomovsky, *Biotechnol. Bioeng.*, 2019, **116**, 1231–1244.
- 10 A. G. Proidakov, *Solid Fuel Chem.*, 2009, **43**, 9–14.
- 11 J. Wang, G. J. Guo, Y. Han, Q. Hou, M. Geng and Z. Zhang, *Fuel*, 2019, **253**, 1247–1255.
- 12 P. Stellacci, L. Liberti, M. Notarnicola and P. L. Bishop, *Chem. Eng. J.*, 2009, **149**, 11–18.
- 13 L. Takacs, *Acta Phys. Pol., A*, 2014, **4**, 1040–1043.
- 14 A. P. Burdukov, V. I. Popov, M. Y. Chernetskiy, A. A. Dekterev and K. Hanjalić, *Appl. Therm. Eng.*, 2015, **74**, 174–181.
- 15 T. M. Chrenkova, *Mechanochemical Activation of Coal*, Nedra, Moscow, 1993.
- 16 J. Liu, X. Jiang, J. Shen and H. Zhang, *Adv. Powder Technol.*, 2014, **25**, 916–925.
- 17 L. Turčániová and P. Baláž, *J. Mater. Synth. Process.*, 2000, **8**, 365–367.
- 18 T. S. Urazova, A. L. Bychkov and O. I. Lomovskii, *Russ. J. Appl. Chem.*, 2014, **87**, 651–655.
- 19 G. Cagnetta, J. Huang and G. Yu, *Crit. Rev. Environ. Sci. Technol.*, 2018, **48**, 723–771.
- 20 J. Webster, M. Lee, L. W. Gurba, M. Manefield and T. Thomas, *Fuel*, 2019, **257**, 116071.
- 21 T. Skripkina, A. Bychkov, V. Tikhova, B. Smolyakov and O. Lomovsky, *Environ. Technol. Innov.*, 2018, **11**, 74–82.
- 22 T. S. Skripkina, A. L. Bychkov, B. S. Smolyakov and O. I. Lomovsky, *Water Resour.*, 2019, **46**, 242–248.
- 23 T. S. Skripkina, A. L. Bychkov, V. D. Tikhova and O. I. Lomovsky, *Solid Fuel Chem.*, 2018, **52**, 356–360.
- 24 P. H. Emmett, S. Brunauer and E. Teller, *J. Am. Chem. Soc.*, 1938, **60**, 309–319.
- 25 S. J. Gregg, K. S. W. Sing and H. W. Salzberg, *J. Electrochem. Soc.*, 1967, **114**, 279.
- 26 H. Asgar, K. M. Deen, U. Riaz, Z. U. Rahman, U. H. Shah and W. Haider, *Mater. Chem. Phys.*, 2018, **206**, 7–11.
- 27 M. W. Haenel, *Fuel*, 1992, **71**, 1211–1223.
- 28 J. Cai, S. Yang, X. Hu, W. Song, Q. Xu, B. Zhou and Y. Song, *Fuel*, 2019, **253**, 339–348.
- 29 E. Avvakumov, M. Senna and N. Kosova, *Soft Mechanochemical Synthesis: A Basis for New Chemical Technologies*, Springer Science & Business Media, Boston, 2001.
- 30 I. A. Tumanov, A. A. L. Michalchuk, A. A. Politov, E. V. Boldyreva and V. V. Boldyrev, *Dokl. Chem.*, 2017, **472**, 17–19.
- 31 B. Riss-Yaw, T. X. Métro, F. Lamaty and F. Coutrot, *RSC Adv.*, 2019, **9**, 21587–21590.
- 32 J. Sun, Y. Yang, Y. Guo, Y. Xu, W. Li, C. Zhao, W. Liu and P. Lu, *Fuel*, 2018, **222**, 334–342.
- 33 V. V. Boldyrev, *Powder Technol.*, 2002, **122**, 247–254.
- 34 W. L. Suchanek, P. Shuk, K. Byrappa, R. E. Riman, K. S. TenHuisen and V. F. Janas, *Biomaterials*, 2002, **23**, 699–710.
- 35 N. V. Kosova, A. K. Khabibullin and V. V. Boldyrev, *Solid State Ionics*, 1997, **101**, 53–58.

- 36 P. Shuk, W. L. Suchanek, T. Hao, E. Gulliver, R. E. Riman, M. Senna, K. S. TenHuisen and V. F. Janas, *J. Mater. Res.*, 2001, **16**, 1231–1234.
- 37 F. Liu, H. Guo, Q. Wang, R. Haider, M. A. Urynowicz, P. H. Fallgren, S. Jin, M. Tang, B. Chen and Z. Huang, *Fuel*, 2019, **237**, 1209–1216, DOI: 10.1016/j.fuel.2018.10.043.
- 38 J. Gołowski, J. Sekulska-Nalewajko, B. Strzelecki and I. Romanowska, *Fuel*, 2019, **256**, 115927.
- 39 P. R. Santhanam and E. L. Dreizin, *Powder Technol.*, 2012, **221**, 403–411.
- 40 G. Cagnetta, J. Huang, B. Wang, S. Deng and G. Yu, *Chem. Eng. J.*, 2016, **291**, 30–38.
- 41 H. El Briak-BenAbdeslam, M. P. Ginebra, M. Vert and P. Boudeville, *Acta Biomater.*, 2008, **4**, 378–386.